Imaging Science in Dentistry 2017; 47: 189-97
https://doi.org/10.5624/isd.2017.47.3.189

Quantitative assessment of image artifacts from root filling materials on CBCT scans made using several exposure parameters

Katharina Alves Rabelo[1], Yuri Wanderley Cavalcanti[1], Martina Gerlane de Oliveira Pinto[1], Saulo Leonardo Sousa Melo[2], Paulo Sérgio Flores Campos[3], Luciana Soares de Andrade Freitas Oliveira[4], Daniela Pita de Melo[1,*]

[1]*Department of Oral Diagnosis, State University of Paraíba, Campina Grande, Brazil*
[2]*Department of Oral Pathology, Radiology and Medicine, University of Iowa, Iowa City, USA*
[3]*Department of Oral Diagnosis, Federal University of Bahia, Salvador, Brazil*
[4]*Department of Health Technology and Biology, Division of Radiology, Federal Institute of Bahia, Salvador, Brazil*

ABSTRACT

Purpose: To quantify artifacts from different root filling materials in cone-beam computed tomography (CBCT) images acquired using different exposure parameters.

Materials and Methods: Fifteen single-rooted teeth were scanned using 8 different exposure protocols with 3 different filling materials and once without filling material as a control group. Artifact quantification was performed by a trained observer who made measurements in the central axial slice of all acquired images in a fixed region of interest using ImageJ. Hyperdense artifacts, hypodense artifacts, and the remaining tooth area were identified, and the percentages of hyperdense and hypodense artifacts, remaining tooth area, and tooth area affected by the artifacts were calculated. Artifacts were analyzed qualitatively by 2 observers using the following scores: absence (0), moderate presence (1), and high presence (2) for hypodense halos, hypodense lines, and hyperdense lines. Two-way ANOVA and the post-hoc Tukey test were used for quantitative and qualitative artifact analysis. The Dunnet test was also used for qualitative analysis. The significance level was set at $P < .05$.

Results: There were no significant interactions among the exposure parameters in the quantitative or qualitative analysis. Significant differences were observed among the studied filling materials in all quantitative analyses. In the qualitative analyses, all materials differed from the control group in terms of hypodense and hyperdense lines ($P < .05$). Fiberglass posts did not differ statistically from the control group in terms of hypodense halos ($P > .05$).

Conclusion: Different exposure parameters did not affect the objective or subjective observations of artifacts in CBCT images; however, the filling materials used in endodontic restorations did affect both types of assessments. ***(Imaging Sci Dent 2017; 47: 189-97)***

KEY WORDS: Imaging, Three-Dimensional; Cone-Beam Computed Tomography; Artifacts

Introduction

Computed tomography (CT) provides precise reconstructions of alveolar bone, but not for teeth, because of its limited spatial resolution and artifacts derived from beam hardening, scatter radiation, quantum noise (Poisson noise), and photon starvation caused by metallic restorations, crowns, brackets, implants, and metal root fillings.[1-4] Cone-beam CT (CBCT), developed for the oral and maxillofacial region in 1998,[5] has become an alternative to CT in dental practice,[1] providing similar images to CT at a lower cost and reduced radiation dose.[4]

Both CT and CBCT use the same image reconstruction principle, referred to as back-projection, with the addition of different algorithms depending on the technique.[6] CT and CBCT are affected by metallic objects, which disturb

Received February 11, 2017; Revised June 3, 2017; Accepted June 7, 2017
*Correspondence to : Prof. Daniela Pita de Melo
Rua Baraúnas, 351, Bairro Universitário, Campina Grande-PB, 58429-500, Brazil
Tel) 55-83-3315-3300, Fax) 55-83-3315-3300, E-mail) danipita@gmail.com

Imaging Science in Dentistry · pISSN 2233-7822 eISSN 2233-7830

the electronic reconstructions to different degrees[6] by causing distortions in the reconstructed data.[1,7] These alterations in the reconstructed images, commonly known as artifacts, are not present in the original object and can be observed as streaking artifacts,[4] metal object-internal hypodense areas (cupping artifacts)[8] or hypodense halos caused by metallic structures.[7] Therefore, artifacts can impair diagnosis, treatment planning, and follow-up analysis because the region of interest may not be properly visualized.[1] Moreover, the effects of metal artifacts may be even more pronounced in CBCT due to its inferior contrast resolution compared to CT.[4]

Previous studies have evaluated the presence and the effects of artifacts originating from metallic root fillings, using both qualitative[7,8] and quantitative methods.[1,3,9,10] Although Bezerra et al.[9] proposed a quantitative evaluation of artifact formation by means of pixel value measurement, it is known that the gray level is non-uniform in CBCT images, which contributes to artifact formation in reconstructed images[5] and makes pixel quantification inaccurate. Beam hardening and scatter radiation may affect gray-level non-uniformity on CBCT, as neither is accounted for in the mathematics of image formation.[5] Other factors that also contribute to gray-level non-uniformity are object position, imaging parameters, and the CBCT device used for image acquisition.[11-13] According to Hunter and McDavid,[5] this gray-level non-uniformity throughout the field of view (FOV) prevented the use of CBCT for quantitative analyses.

In a previous study, the influence of different exposure parameter protocols on CBCT images using different root filling materials was analyzed through a diagnostic evaluation, while artifact formation was investigated subjectively; the lowest exposure parameters subjectively presented the worst images in terms of artifacts, but this did not interfere with fracture detection.[14] According to Pauwels et al.,[1] subjective artifact evaluation could be useful for assessing artifact reduction and its effects on diagnosis, but they were not able to evaluate the performance of different devices and protocols, so such a process was not indicated for quality control.

Although different approaches have been used to quantify metal artifacts, the most relevant studies used phantoms with no surrounding tissue[1,10] or a non-dentate mandible,[3] so that the artifact could be precisely measured. An absence of surrounding tissue may be ideal for artifact quantification, but it does not reflect clinical reality. For that reason, the aim of this study was to quantify hyperdense and hypodense artifacts in CBCT images using different exposure parameters and different root filling materials in an ex vivo phantom.

Materials and Methods

This study protocol was approved by the Institutional Review Board in accordance with the Helsinki Declaration (#39088714.2.0000.5187).

Sample preparation

Fifteen single-rooted human teeth, extracted for therapeutic reasons, were included in the sample. The teeth were inspected by transillumination and digital radiography (No. 2 Digora Optime phosphor plate, Soredex, Tuusula, Finland) to exclude those with root fractures, canal obliteration, root resorption, or any other anomaly. Tooth crowns were removed at the cementoenamel junction and root canals were standardized using the ProTaper rotary system (Dentsply Maillefer, Ballaigues, Switzerland) to size F5.

Type III gold-alloy (MaxiGold XH, Ivoclar Vivadent, Schaan, Liechtenstein) and pre-fabricated fiberglass (Fibercone, RTD, Lançon-Provence, France) posts were cast in all evaluated teeth. ProTaper F5 gutta-percha cones (Protaper Universal F5 Gutta Percha Points, Denstsply, Ballaigues, Switzerland) were also selected. All posts and gutta-percha cones were passively well-fitted and non-cemented. Periapical radiographs were obtained to validate the gutta-percha cone, fiberglass post, and metallic post adaptation, one at a time, in the root canal of each tooth.

Image acquisition

A 0.2-mm layer of wax was used to coat each tooth. Each tooth was placed individually in an empty maxillary anterior socket of a partially dentate dry human skull. The skull was coated with a 5-mm-thick layer of wax and then immersed in a styrofoam box filled with water to provide images similar to clinical situations by simulating soft tissue (Fig. 1).[14]

CBCT images were acquired on a CS 9000 3D unit (Carestream Dental, Rochester, NY, USA) using the following exposure protocols: (1) 74 kV/12 mA; (2) 74 kV/10 mA; (3) 74 kV/8 mA; (4) 74 kV/6.3 mA; (5) 70 kV/12 mA; (6) 70 kV/10 mA; (7) 70 kV/8 mA; and (8) 70 kV/6.3 mA. The voxel size and FOV were fixed at 0.100 mm and 5 cm × 3.75 cm, respectively, for all exposure protocols.

Each tooth was scanned 4 times using each protocol. The first scan was made without any intracanal material, and it was followed by scans with a gutta-percha cone,

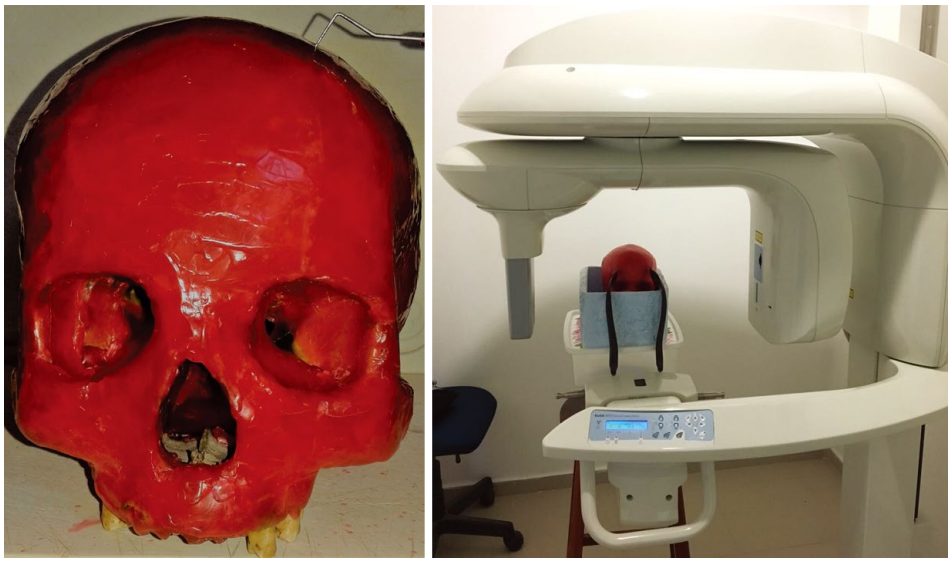

Fig. 1. A human skull is coated with a 5-mm-thick layer of wax to simulate soft tissue, then immersed in a in a styrofoam box filled with water. The skull is positioned in the cone-beam computed tomography unit while taking the image.

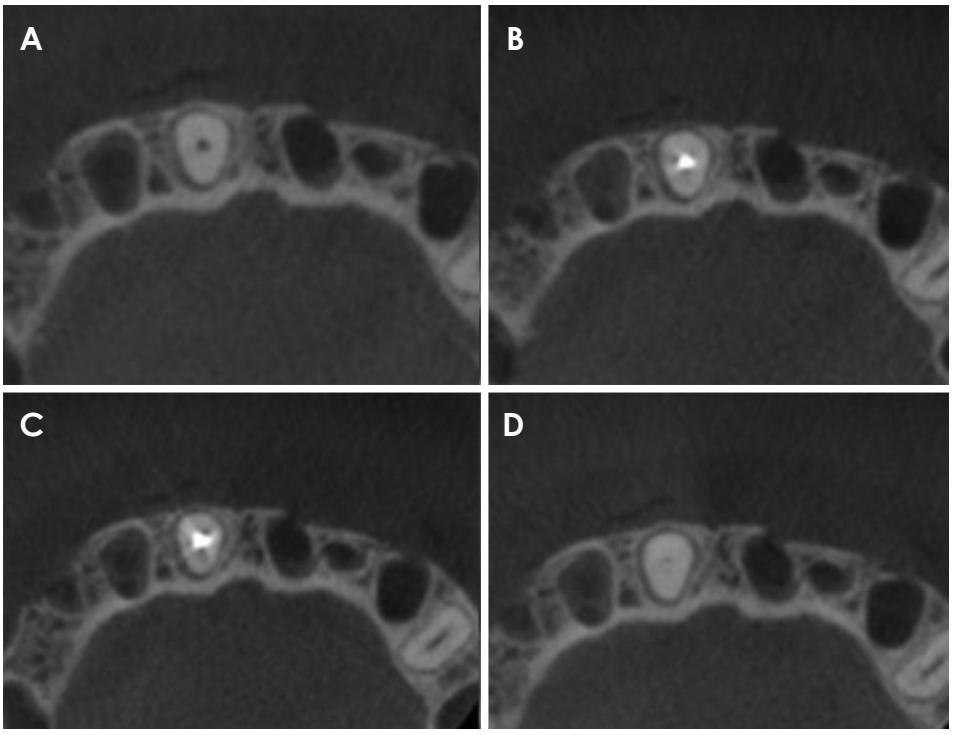

Fig. 2. Axial cone-beam computed tomography images show a tooth with the 4 root filling conditions that were studied. A. Empty filling. B. ProTaper F5 gutta-percha point. C. Type III gold-alloy post. D. Prefabricated fiberglass post.

a fiberglass post, and a gold alloy post placed in the root canal (Fig. 2). The resultant dataset was exported as Digital Imaging and Communications in Medicine (DICOM) files and saved with a code corresponding to the tooth, root filling status, and parameter protocol used.

Artifact quantification

Each DICOM file was read on the scanner's native software (CS3D imaging software, v3.1.9; Carestream Dental Inc., Rochester, NY, USA) and the most representative axial slice of the middle third of the studied root was selected and exported as a DICOM image. DICOM datasets were decompressed with the CS3D imaging software tool before they were imported into the software, because GNU Image Manipulation Program (GIMP) (version 2.8.14. The GIMP Team, USA https://www.gimp.org/) and ImageJ (National Institutes of Health, Bethesda, USA, http://rsb.info.nih.gov/ij/) cannot open compressed

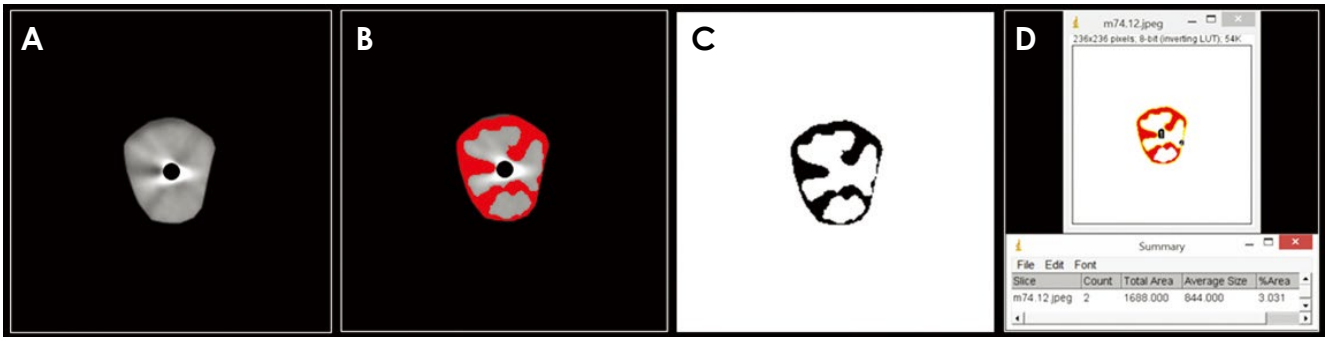

Fig. 3. Quantification of the hypodense area of image artifacts is performed with a limited threshold using ImageJ tools. A. Axial image of the tooth selected for artifact quantification. B. Hyperdense area selected based on the manually determined threshold range. C. Hyperdense area determined by ImageJ selection according to the threshold range. D. Resultant value of the selected area.

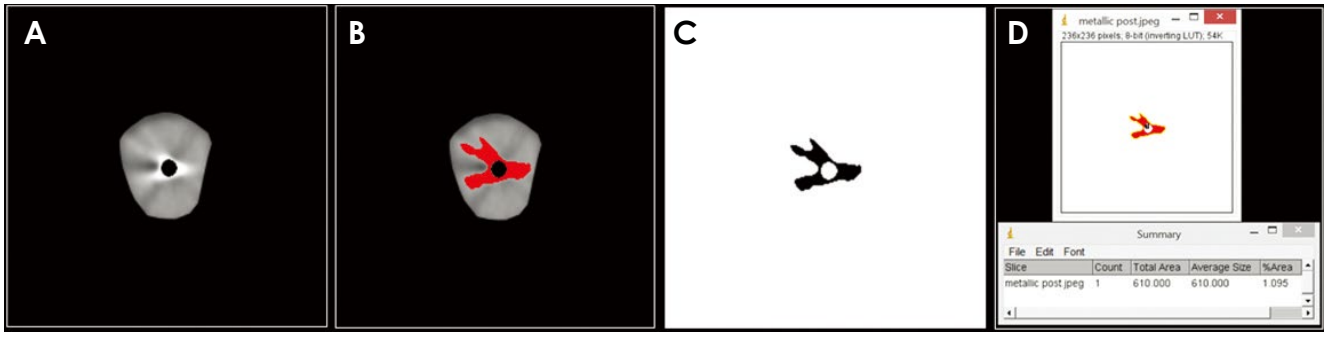

Fig. 4. Quantification of hyperdense of image artifacts is performed with a limited threshold using ImageJ tools. A. Axial image of the tooth selected for artifact quantification. B. Hypodense area selected based on the manually determined threshold range. C. Hypodense area determined by ImageJ selection according to the threshold range. D. Resultant value of the selected area.

images.[1] The axial image was imported into GIMP, and a fixed region of interest (ROI) encompassing the entire root area, except for the root canal space and its corresponding filling material, was selected using the 'analyze particles' and 'bare outlines' tools. The removal of the filling material was performed manually based on the empty tooth images (CBCT images obtained of the tooth without any filling material) given that no standardized segmentation method was appropriate.[1]

The resulting ROI images were set to an 8-bit scale (256 gray values), saved with a black background, and imported to ImageJ version 1.48 (National Institutes of Health, Bethesda, MD, USA, http://rsb.info.nih.gov/ij/). Within the selected ROI, the standard deviation of all pixel values was determined. The threshold tool of ImageJ was used to determine the hypodense areas of image artifacts with a limited threshold according to the evaluated image pixel values (a minimum of 2 and a maximum of 159 pixels) (Fig. 3). The same steps were used for hyperdense artifact quantification, except that the threshold of the hyperdense artifacts was different (a minimum of 158 and a maximum of 255 pixels) (Fig. 4). After establishing the artifact areas, the remaining tooth areas were also calculated for all teeth based on the total area of the empty tooth (cross-sectional tooth images without any restorative material in the root canal).

For the objective analysis, 480 evaluations were done, corresponding to 15 teeth scanned using 8 different parameters and 3 filling materials, as well as a control group (empty teeth without any restorative material within the root canal). As the limited threshold of the fiberglass posts' density was equal to the threshold of the remaining tooth area, the operator could not distinguish it from the teeth or separate it using the software tools. The hyperdense and hypodense artifact images were not detected in the images of fiberglass posts, so it was not possible to carry out the quantitative analysis in this group. The control group behaved like the fiberglass group. The empty teeth images (control group) were used to measure the total teeth areas.

The areas corresponding to hypodense artifacts, hyperdense artifacts, and the remaining teeth area were obtained. Calculations based on the images of teeth without artifacts (control) were then made in order to calculate the percentages of hypodense and hyperdense artifacts, as well as the percentage of tooth images without alteration (remaining teeth). This calculation was based on the value of each area divided by the total area of the tooth. The percentage of the tooth image that was not affected by the filling material was calculated by dividing the remaining tooth area by the total tooth area of the control tooth image (empty tooth image).

Qualitative analysis of artifacts

Two trained and calibrated oral and maxillofacial radiologists individually performed qualitative analysis to evaluate the artifact patterns in the CBCT images.

Eight DVDs (DVD-R 4.7 GB; Sony, Zaventem, Belgium) with 30 acquisitions in a random order were given to the observers. The images were visualized using CS 3D Imaging Software (Carestream Dental, Rochester, NY, USA), displayed on a 24-inch Ultra Sharp DELL (24 UltraSharp Monitor; U2412M, Dell Inc, Austin, USA) color monitor in a quiet room with dimmed light. A maximum of 15 volumes were evaluated per day with a minimum interval of 24 hours. For the subjective analysis, 480 volumes were assessed per observer, corresponding to 15 teeth scanned using 8 different parameters and 3 filling materials, as well as a control group composed of images of empty teeth. Zooming, brightness, and contrast settings were left to each observer's preference.

Gutta-percha, fiberglass, and gold alloy posts artifacts were graded to define the artifact pattern using an adaptation of the scores developed by Vasconcelos et al.,[7] as follows: absence (0), moderate presence (1), or high presence (2) for hypodense halos (dark bands), thin hypodense lines (dark lines), and hyperdense lines (streaks). The empty teeth images were also graded as a control group due to the possible effects of the different parameters on artifact formation.

Data analysis

For quantitative artifact analysis, data were computed and analyzed using SPSS version 20 (IBM Corp., Armonk, NY, USA). The exposure parameters for CBCT image acquisitions (kV and mA) and the material used for intracanal filling (metal post and gutta-percha) were used as independent variables. The percentage of image artifacts, as well as the percentage of remaining tooth in image and the percentage of tooth image not affected by the filling material were considered the response variables.

Two-way analysis of variance (ANOVA) was performed to detect statistically significant factors, or interactions between them, that interfered with the response variables. Post-hoc comparisons for CBCT exposure parameters were done using the Tukey honest significant difference (HSD) test. The difference between metal and gutta-percha was analyzed using the Tukey independent test. The significance level was set at 5% ($P < .05$).

For the qualitative artifact analysis, since scores were used, data were analyzed using 2-way ANOVA, followed by the post hoc Tukey test, to detect statistically significant factors or interactions between them that interfered with the response variables. The Dunnet test was also used to compare the presence of hypodense lines, bands, and streaks between the images obtained using different parameters and the control group images acquired with the exposure protocol of 74 kV and 12 mA. The significance level was set at 5% ($P < .05$).

Results

The kappa coefficient values for the interobserver analysis were 0.867 for hypodense halos, 0.946 for hypodense lines, and 0.981 for hyperdense lines (streaks) in the qualitative analysis.

For the qualitative analysis, statistically significant differences were only found between the filling materials, but not among the exposure parameters analyzed (Table 1). The mean scores for hypodense halos were 0.00 for the fiberglass post and control group, 0.571 for gutta-percha, and 1.804 for metal posts. For hypodense lines, the mean scores were 0.037 for the control group, 0.342 for fiberglass posts, 1.083 for gutta-percha, and 1.913 for metal posts. For hyperdense lines, the mean scores were 0.033 for the control group, 0.333 for fiberglass posts, 0.879 for gutta-percha, and 1.916 for metal posts.

For the quantitative analysis, no statistically significant interactions were found among the exposure parameters that were studied, considering all the response variables analyzed. Statistically significant differences were observed for the filling materials, which significantly influenced the percentage of hypodense and hyperdense artifacts, as well as that of the tooth image preserved (both percentage of remaining tooth in image and the percentage of tooth image not affected by the filling material). No influence of CBCT exposure parameters (kV and mA) was detected for any variable that was considered (Table 2).

Table 1. Distribution of qualitative evaluations regarding the presence of hypodense halos, hypodense lines, and hyperdense lines, according to the type of materials and exposure parameters

Materials	Parameters	Hypodense halo			Hypodense lines			Hyperdense lines (streaks)		
		Absence	Moderate presence	High presence	Absence	Moderate presence	High presence	Absence	Moderate presence	High presence
Empty (Control)	74 kV, 12 mA	30	0	0	30	0	0	30	0	0
	74 kV, 10 mA	30	0	0	30	0	0	30	0	0
	74 kV, 8 mA	28	0	2	28	0	2	28	0	2
	74 kV, 6.3 mA	28	0	2	28	0	2	28	0	2
	70 kV, 12 mA	30	0	0	30	0	0	30	0	0
	70 kV, 10 mA	30	0	0	30	0	0	30	0	0
	70 kV, 8 mA	30	0	0	30	0	0	30	0	0
	70 kV, 6.3 mA	30	0	0	29	1	0	30	0	0
Gutta-percha*	74 kV, 12 mA	15	15	0	2	27	1	7	23	0
	74 kV, 10 mA	13	17	0	0	29	1	6	24	0
	74 kV, 8 mA	14	16	0	0	27	3	6	21	3
	74 kV, 6.3 mA	16	14	0	0	28	2	7	21	2
	70 kV, 12 mA	14	12	4	0	25	5	5	21	4
	70 kV, 10 mA	12	16	2	0	27	3	4	24	2
	70 kV, 8 mA	13	15	2	0	27	3	6	22	2
	70 kV, 6.3 mA	14	16	0	0	26	4	4	23	3
Metal post*	74 kV, 12 mA	0	8	22	0	5	25	0	4	26
	74 kV, 10 mA	1	8	21	0	2	28	0	2	28
	74 kV, 8 mA	0	7	23	0	2	28	0	2	28
	74 kV, 6.3 mA	0	7	23	0	2	28	0	2	28
	70 kV, 12 mA	0	4	26	0	2	28	0	2	28
	70 kV, 10 mA	0	2	28	0	2	28	0	2	28
	70 kV, 8 mA	0	3	27	0	2	28	0	2	28
	70 kV, 6.3 mA	1	4	25	1	2	27	1	2	27
Fiberglass post*	74 kV, 12 mA	30	0	0	18	12	0	20	10	0
	74 kV, 10 mA	30	0	0	20	10	0	20	10	0
	74 kV, 8 mA	30	0	0	20	10	0	20	10	0
	74 kV, 6.3 mA	30	0	0	20	10	0	20	10	0
	70 kV, 12 mA	30	0	0	20	10	0	20	10	0
	70 kV, 10 mA	30	0	0	20	10	0	20	10	0
	70 kV, 8 mA	30	0	0	20	10	0	20	10	0
	70 kV, 6.3 mA	30	0	0	20	10	0	20	10	0

*$P < .05$ compared with the control (empty)

Discussion

An artifact is any distortion or error in the image that has no relationship to the subject being studied,[15] and for CT images specifically, artifacts are any systematic discrepancies between the CT numbers in the reconstructed image and the expected CT numbers based on the true coefficient of linear attenuation of the studied object.[5,16] Those artifacts appear in CT images as dark bands, dark lines, and streaks.

A diverse range of artifacts has been observed in CT and CBCT images, due to effects such as beam hardening, scattering, quantum noise (poison noise) and photon starvation. These effects result in different types of image degradation, which can range from streaks radiating from the metallic object to darkening of its surrounding area and even the total loss of gray values between proximate metallic objects.[1]

As metal artifacts may impair diagnosis, previous studies have evaluated the presence of metal artifacts in different scanning situations;[1,3,6,7,11,14,17-19] and the possibility of reducing their presence using different filters and artifact reduction algorithms.[5,9,20-23]

According to Chindasombatjareon et al.,[10] higher tube voltages (kV) were associated with smaller artifact areas; however, increasing the tube current (mA) had no predictable effect on the artifact area, in agreement with a previous study.[24] However, Barrett and Keat[17] stated that one could minimize the effects of photon starvation by increasing tube current (mA), but at the patient's cost,

Table 2. Percentage of hypodense artifacts, hyperdense artifacts, and dental image preserved values for the studied exposure parameters and filling materials.

Parameters	Remaining tooth in image		Hypodense artifact in image		Hyperdense artifact in image (streaks)		Tooth image not affected by the filling material	
	Metal (A)	Gutta (A)	Metal (A)	Gutta (B)	Metal (A)	Gutta (B)	Metal (A)	Gutta (B)
74 kV, 12 mA	48.4 ± 0.9^{a}	47.3 ± 1.0^{b}	35.6 ± 1.0^{a}	39.9 ± 1.1^{b}	16.0 ± 0.7^{a}	12.8 ± 0.4^{b}	58.7 ± 1.9^{a}	54.0 ± 1.6^{b}
74 kV, 10 mA	48.5 ± 1.0^{a}	46.4 ± 0.8^{b}	34.6 ± 1.0^{a}	40.0 ± 0.8^{b}	16.9 ± 0.6^{a}	13.5 ± 0.4^{b}	58.8 ± 1.5^{a}	50.4 ± 1.2^{b}
74 kV, 8 mA	47.3 ± 1.2^{a}	47.4 ± 1.0^{b}	35.8 ± 1.1^{a}	39.3 ± 0.9^{b}	16.8 ± 0.5^{a}	13.2 ± 0.4^{b}	59.4 ± 1.7^{a}	54.4 ± 1.9^{b}
74 kV, 6.3 mA	50.1 ± 1.1^{a}	46.8 ± 1.2^{b}	32.7 ± 1.1^{a}	39.0 ± 1.3^{b}	17.1 ± 0.6^{a}	14.1 ± 0.5^{b}	64.3 ± 1.9^{a}	57.1 ± 2.8^{b}
70 kV, 12 mA	50.0 ± 1.1^{a}	48.1 ± 1.2^{b}	32.8 ± 1.2^{a}	38.5 ± 1.0^{b}	17.2 ± 0.6^{a}	13.3 ± 0.4^{b}	62.8 ± 1.4^{a}	52.9 ± 1.7^{b}
70 kV, 10 mA	49.7 ± 0.9^{a}	48.5 ± 0.9^{b}	32.7 ± 0.9^{a}	36.7 ± 1.0^{b}	17.6 ± 0.6^{a}	14.8 ± 0.5^{b}	62.6 ± 1.5^{a}	54.1 ± 1.8^{b}
70 kV, 8 mA	51.8 ± 0.9^{a}	46.0 ± 0.7^{b}	32.5 ± 1.0^{a}	40.1 ± 0.6^{b}	15.7 ± 0.6^{a}	13.9 ± 0.5^{b}	67.5 ± 1.9^{a}	53.7 ± 1.5^{b}
70 kV, 6.3 mA	50.6 ± 0.9^{a}	46.7 ± 0.7^{b}	32.6 ± 1.0^{a}	41.1 ± 0.8^{b}	16.7 ± 0.5^{a}	12.1 ± 0.4^{b}	65.3 ± 1.6^{a}	54.3 ± 1.3^{b}

Uppercase letters indicate a statistically significant difference between materials ($P < .05$). Different lowercase superscript letters within the same material indicate statistically significant differences among parameters ($P < .05$).

since an unnecessary dose was administered when the beam passed through less attenuating parts. Shulze et al.[25] found visible artifact reduction in the range between 120 and 140 kV, but this difference did not effectively reduce the artifacts in clinical situations. In this study, different scanning parameters did not affect the perception of artifacts in the images as assessed objectively or subjectively; however, the maximum tube voltage used was 72 kV and the maximum tube current was 12 mA, lower values than a previous study.[10] Using higher levels of kV and mA, leading to a greater radiation dose, to avoid image artifacts was not justified when using CS9000 3D.

The cupping artifact, a type of beam-hardening artifact, has been described in previous studies, but controversy remains regarding it. According to Vasconcelos et al.,[7] the cupping artifact is a distortion of the metal object. Previous studies[8,17] described a beam-hardening cupping effect; as the beams became harder, their attenuation decreased, so the beams were more intense when they reached the detectors than would be expected if they had not been hardened. With a cylindrical phantom, a profile of the CT numbers would display a characteristic cupped shape, affecting the metal and non-metal regions in the reconstructed image. This effect was more prominent in large-FOV image acquisitions,[17] and did not cause a distortion in the metal image at its edge, but did cause a distortion in its inner portion. In CBCT images from small FOV scanners, the cupping artifact was indistinguishable from other artifacts in the images.

To avoid confusion among observers trying to distinguish among various artifact types, the authors decided that it was best to divide artifacts into general categories referring to how they appeared in the images: hypodense halos, hypodense lines, and hyperdense lines. Vasconcelos et al.[7] reported better interobserver and intraobserver agreement for streaks and hypodense halo artifacts than for cupping artifacts, varying from moderate to almost perfect. This could be due to the difficulty of distinguishing cupping artifacts. In this study, the agreement was almost perfect for all subjectively evaluated artifact categories.

Artifacts can always be observed in the vicinity of titanium implants. When compared to situations where implants are not present, increased gray values are present in the buccal and lingual proximity of all implant sites; and regions with reduced gray values can be observed along the axis of the jaw.[3] That can be explained by the fact that CT images are acquired with polychromatic X-ray sources, which means that when an X-ray goes through metal objects, low-energy X-ray photons are absorbed, and the remaining high-energy photons are not easily attenuated, which leads to beam-hardening effects such as dark bands and lines between metal structures.[8] This type of artifact can be commonly seen in dental images between 2 implants or 2 metal posts positioned in the same jaw, in close proximity to each other.[26]

In this study, hypodense artifact areas were larger in gutta-percha images than in metal post images for the quantitative analysis; however, in the qualitative analysis, metal posts had a higher score for hypodense halos and hypodense lines. The hypodense artifact areas for metal posts varied from 32.5% to 35.6% of the total tooth images, indicating a substantial image loss due to hypodense metal artifacts, in agreement with previous studies.[1,7,10] Hypodense artifacts may mimic disease. For example, when they originate from root-canal filling material, they can mimic root fractures, whereas dark bands around dental implants can mimic loss of osseointegration.[20] Thus,

such artifacts can negatively affect the accuracy of the diagnosis if one is not familiar with their occurrence in images where high-density materials are present.

Human jaws are heterogeneous structures composed of diverse types of hard and soft tissues.[3] In this study, the soft tissues were simulated using wax, water, and a styrofoam box, which may be a limitation, as it is known that the density response in CBCT scanners depends on the total mass of all structures positioned inside and outside the FOV;[3,13] however, trying to simulate soft tissue so the images will be as similar as possible to patients' images makes this methodological approach more realistic than using acrylic phantoms alone. The presence of anatomical structures influences the gray-value measurements of the jaw bones in CBCT due to the heterogeneity of the human jaws.

Chindasombatjareon et al.[10] compared CBCT and CT artifact areas using an acrylic phantom and metal cubes of aluminum, titanium, cobalt-chromium alloy, and type IV gold alloy, and found that using the same exposure parameters, the type IV gold alloy metal cube presented larger artifact areas, especially for hyperdense (white) artifacts. The same authors found that CT showed larger artifact areas than CBCT in most conditions; however, for hyperdense artifacts, CBCT images with a low tube current and low tube voltage can present larger artifact areas. In this study, the metal used to manufacture the metal post was a type III gold alloy, which also presented larger hyperdense artifact areas.

Tools in ImageJ have been used before to quantify metal artifacts in CBCT and CT in different ways.[1,9-11,22] This study used an adaptation of the methodology of Pauwels et al.,[1] derived from van der Schaaf et al.,[27] which has been used before to quantify artifact areas.[10,11] The areas and percentages of the tooth affected by hypodense and hyperdense artifacts are relatively accurate when studying the effect of artifacts on image quality due to the nature of CBCT images, in which pixel intensity is heterogeneous, especially in clinical situations where all structures of the oral and maxillofacial region interfere in the CBCT image.[11,12,28]

The cone beam geometry yields additional challenges in artifact reduction compared to CT reconstruction.[1] Bezerra et al.[9] found that activating the Picasso Trio artifact reduction system did indeed reduce artifacts; however, it had a negative impact on vertical root fracture detection in teeth with a metal post. Significant artifact reduction should be based on a special mathematical modeling of the existing physical image acquisition process in place of post-processing of the incorrect results obtained from raw reconstruction algorithms[25] that may in some cases impair diagnosis. Although previous studies[29,30] have found image quality improvements when using artifact reduction algorithms, other studies found similar results between CBCT images with and without artifact reduction algorithms or enhancement filters for different diagnostic purposes,[20,21,31] indicating that the use of metal artifact reduction algorithms cannot be justified.

The quantitative assessment of CBCT artifacts has generally been done in one or more slices, which could be a limitation. The ideal evaluation would incorporate the entire CBCT volume, as is done for the qualitative assessment. Isolating artifacts three-dimensionally has been a challenge. It could be done by means of segmentation, but separating the artifacts from the metal object in this image modality is rather difficult. New segmentation software programs should be tested in order to isolate whole metal artifacts from the whole image volume.

Different exposure parameters did not seem to affect the degree to which artifacts were observed objectively and subjectively in CBCT images; however, the metal post and gutta-percha intracanal filling materials did influence both types of artifact assessments. Three-dimensional quantitative artifact studies are needed to evaluate the artifacts from the whole image volume.

References

1. Pauwels R, Stamatakis H, Bosmans H, Bogaerts R, Jacobs R, Horner K, et al. Quantification of metal artifacts on cone beam computed tomography images. Clin Oral Implants Res 2013; 24 Suppl A100: 94-9.
2. Schulze R, Heil U, Gross D, Bruellmann DD, Dranischnikow E, Schwanecke U, et al. Artefacts in CBCT: a review. Dentomaxillifac Radiol 2011; 40: 265-73.
3. Benic GI, Sancho-Puchades M, Jung RE, Deyhle H, Hämmerle CH. In vitro assessment of artifacts induced by titanium dental implants in cone beam computed tomography. Clin Oral Implants Res 2013; 24: 378-83.
4. Hassan B, Couto Souza P, Jacobs R, de Azambuja Berti S, van der Stelt P. Influence of scanning and reconstruction parameters on quality of three-dimensional surface models of the dental arches from cone beam computed tomography. Clin Oral Investig 2010; 14: 303-10.
5. Hunter AK, McDavid WD. Characterization and correction of cupping effect artefacts in cone beam CT. Dentomaxillofac Radiol 2012; 41: 217-23.
6. Nardi C, Borri C, Regini F, Calistri L, Castellani A, Lorini C, et al. Metal and motion artifacts by cone beam computed tomography (CBCT) in dental and maxillofacial study. Radiol Med 2015; 120: 618-26.
7. Vasconcelos KF, Nicolielo LF, Nascimento MC, Haiter-Neto

F, Bóscolo FN, Van Dessel J, et al. Artefact expression associated with several cone-beam computed tomographic machines when imaging root filled teeth. Int Endod J 2015; 48: 994-1000.
8. Boas FE, Fleischmann D. Evaluation of two iterative techniques for reducing metal artifacts in computed tomography. Radiology 2011; 259: 894-902.
9. Bezerra IS, Neves FS, Vasconcelos TV, Ambrosano GM, Freitas DQ. Influence of the artifact reduction algorithm of Picasso Trio CBCT system on the diagnosis of vertical root fractures in teeth with metal posts. Dentomaxillofac Radiol 2015; 14: 20140428.
10. Chindasombatjaroen J, Kakimoto N, Murakami S, Maeda Y, Furukawa S. Quantitative analysis of metallic artefacts caused by dental metals: comparison of cone-beam and multi-detector row CT scanners. Oral Radiol 2011; 27: 114-20.
11. Bamba J, Araki K, Endo A, Okano T. Image quality assessment of three cone beam CT machines using the SEDENTEXCT CT phantom. Dentomaxillofac Radiol 2013; 42: 20120445.
12. Nackaerts O, Maes F, Yan H, Couto Souza P, Pauwels R, Jacobs R. Analysis of intensity variability in multislice and cone beam computed tomography. Clin Oral Implants Res 2011: 22: 873-9.
13. Bryant JA, Drage NA, Richmond S. Study of the scan uniformity from an i-CAT cone beam computed tomography dental imaging system. Dentomaxillofac Radiol 2008: 37: 365-74.
14. Pinto MGO, Rabelo KA, Sousa Melo SL, Campos PSF, Oliveira LSAF, Bento PM, et al. Influence of exposure parameters on the detection of simulated root fractures in the presence of various intracanal materials. Int Endod J 2017: 50: 586-94.
15. Scarfe WC, Farman AG. What is cone-beam CT and how does it work? Dent Clin North Am 2008; 52: 707-30.
16. Nagarajappa AK, Dwivedi N, Tiwari R. Artifacts: the downturn of CBCT image. J Int Soc Prev Community Dent 2015; 5: 440-5.
17. Barrett JF, Keat N. Artifacts in CT: recognition and avoidance. Radiographics 2004; 24: 1679-91.
18. Bechara B, McMahan CA, Noujeim M, Faddoul T, Moore WS, Teixeira FB, et al. Comparison of cone beam CT scans with enhanced photostimulated phosphor plate images in the detection of root fracture of endodontically treated teeth. Dentomaxillofac Radiol 2013; 42: 20120404
19. Esmaeili F, Johari M, Haddadi P. Beam hardening artifacts by dental implants: comparison of cone-beam and 64-slice computed tomography scanners. Dent Res J (Isfahan) 2013; 10: 376-81.
20. Kamburoglu K, Onder B, Murat S, Avsever H, Yüksel S, Paksoy CS. Radiographic detection of artificially created horizontal root fracture using different cone beam CT units with small fields of view. Dentomaxillofac Radiol 2013: 42: 20120261
21. de Rezende Barbosa GL, Sousa Melo SL, Alencar PN, Nascimento MC, Almeida SM. Performance of an artefact reduction algorithm in the diagnosis of in vitro vertical root fracture in four different root filling conditions on CBCT images. Int Endod J 2016; 49: 500-8.
22. Helvacioglu-Yigit D, Demirturk Kocasarac H, Bechara B, Noujeim M. Evaluation and reduction of artifacts generated by 4 different root-end filling materials by using multiple cone-beam computed tomography imaging settings. J Endod 2016; 42: 307-14.
23. de-Azevedo-Vaz SL, Peyneau PD, Ramirez-Sotelo LR, Vasconcelos Kde F, Campos PS, Haiter-Neto F. Efficacy of a cone beam computed tomography metal artifact reduction algorithm for the detection of peri-implant fenestrations and dehiscences. Oral Surg Oral Med Oral Pathol Oral Radiol 2016; 121: 550-6.
24. Draenert FG, Coppenrath E, Herzog P, Müller S, Mueller-Lisse UG. Beam hardening artefacts occur in dental implant scans with the NewTom cone beam CT but not with the dental 4-row multidetector CT. Dentomaxillofac Radiol 2007; 36: 198-203.
25. Schulze RK, Berndt D, d'Hoedt B. On cone-beam computed tomography artifacts induced by titanium implants. Clin Oral Implants Res 2010; 21: 100-7.
26. Jaju PP, Jain M, Singh A, Gupta A. Artefacts in cone beam CT. Open J Stomatol 2013; 3: 292-7
27. van der Schaaf I, van Leeuwen M, Vlassenbroek A, Velthuis B. Minimizing clip artifacts in multi CT angiography of clipped patients. AJNR Am J Neuroradiol 2006; 27: 60-6.
28. Araki K, Okano T. The effect of surrounding conditions on pixel value of cone beam computed tomography. Clin Oral Implants Res 2013; 24: 862-5.
29. Bechara BB, Moore WS, McMahan CA, Noujeim M. Metal artefact reduction with cone beam CT: an in vitro study. Dentomaxillofac Radiol 2012; 41: 248-53.
30. Bechara B, McMahan CA, Geha H, Noujeim M. Evaluation of a cone beam CT artefact reduction algorithm. Dentomaxillofac Radiol 2012; 41: 422-8
31. Ferreira LM, Visconti MA, Nascimento HA, Dallemolle RR, Ambrosano GM, Freitas DQ. Influence of CBCT enhancement filters on diagnosis of vertical root fractures: a simulation study in endodontically treated teeth with and without intracanal posts. Dentomaxillofac Radiol 2015; 44: 20140352